Vessel Tracking in Peripheral CTA Datasets – An Overview

Petr Felkel, Rainer Wegenkittl
VRVis Center, Austria, *www.vrvis.at*
Donau-City-Straße 1, A-1220 Vienna
petr.felkel|rainer.wegenkittl@vrvis.at

Armin Kanitsar
ICGA, Vienna University of Technology
Favoritenstraße 9-11, A-1040 Vienna
armin.kanitsar@cg.tuwien.ac.at

Abstract

In this paper, we describe the results of the literature review focused on the peripheral vessel segmentation in 3D medical datasets, acquired by Computer tomography angiography (CTA) of the human leg.

The fundamental aim of such a segmentation task is a robust method for the detection of main vessels in the leg that simultaneously preserves the vessel calcification (the sediment is called plaque) and allows localization of vessel narrowings (called stenoses). This segmentation has to be free from artifacts, i.e., without false detections of stenoses and without false omitting of any stenotic part. The paper collects seven methods applicable for vessel segmentation.

1. Introduction

The aim of the running project is to develop a fast and robust method for vessel and calcification segmentation, which requires a minimum of user interaction or concentrates the interaction into a minimal number of interventions. The method will be used for diagnosis of peripheral arterial occlusive disease (PAOD), a serious disease of modern ages, which can be treated by surgery, if the details about vessels and calcifications are known. The input 3D datasets are acquired by Computer Tomography Angiography (CTA).

The aim of this paper is a literature research on the topic of vessel segmentation and information about the preliminary tests of interesting methods. It gives an overview of methods dealing with different kinds of vessel segmentation, i.e., not only with peripheral vessels and not only for CTA, as described later. The reasons are twofold: Firstly, only very few articles about CTA exist (or have been found by the authors), and secondly, the principles of 3D segmentation methods from different modalities can be adapted for the goal of the CTA segmentation.

The presented text has the following structure: In Section 2, we briefly characterize the acquisition technique, nine datasets available for testing and the appearance of vessels in the dataset. In Section 3, we describe the methods for vessel segmentation found up to now. In Section 4, we discuss experiences and potentials of each method for the task of peripheral vessels CTA segmentation. Conclusions follow in Section 5.

2. Data Acquisition and Description

Computer tomography angiography (CTA) reconstructs a whole 3D volume from a large amount of X-ray projections. The main arguments for CTA in the diagnosis of PAOD are its non-invasiveness, ability to visualize calcification, lower costs of the whole examination, (currently) better spatial resolution than magnetic resonance angiography (MRA), better availability of CTA compared to MRA, and less amount of contraindications (e.g., metal foreign bodies). The first three arguments are essential also in comparison to the current "gold standard technique"—digital subtraction angiography (DSA).

On the other hand, the amount of data produced by CTA is huge (typically about 512x512x(900–1500) slices, which occupy 450–750 MB of memory). To be able to apply this technique in clinical praxis, such amount of data can not be processed manually and a fast and robust vessel tracking method is necessary.

The tracking method has to take the following aspects into account. The signal from vessels enhanced by an injection of the contrast agent is not homogeneous—one reason is the soft and calcified plaque present in the vessels, which blocks the distribution of the contrast agent, second is the quality of the injection protocol. The scanning resolution causes a partial volume artifact (PVA), when smaller structures share one sampling voxel and their "average" variable is reported. The density values of enhanced vessels overlap with values of low density bone and marrow, the same is true also for calk and bone. The vessel diameter varies drastically, from 45 in abdomen down to 1 voxel in the lower part of the leg. Complications cause also the spatial vicinity of vessel and bone and a fuzzy border between the vessel

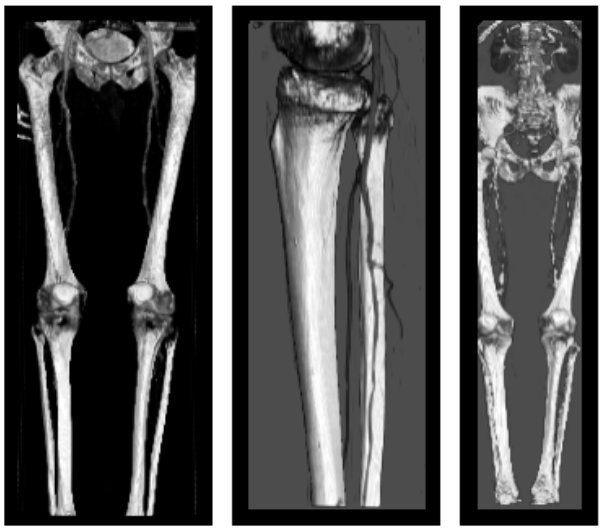

1 2 3

Figure 1. First three datasets in a 3D view

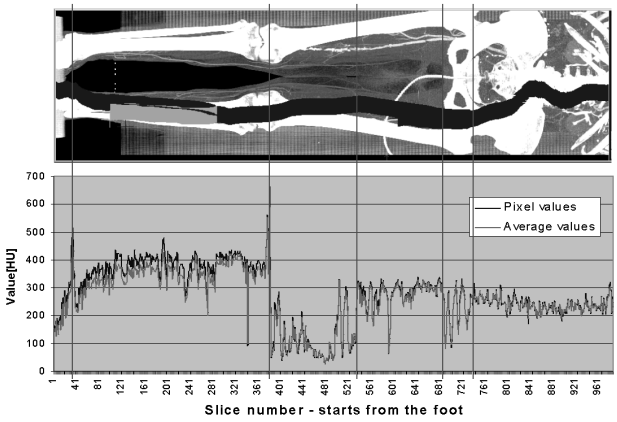

Figure 2. Topogram image of dataset No. 8 with a dark line indicating the manually segmented vessel of the left leg and the voxel density values along the vessel together with the average values of density from a 3x3 surrounding of the center-path

and the bone.

We have tested four of the the algorithms on nine datasets in sizes from 169 to 1134 slices (a typical CTA dataset has 900–1500 slices), representing the typical covered volume of $(250 \text{ to } 380)^2 \times (500 \text{ to } 1000)\ mm^3$. Slice resolution (slice pixel size) from 0.25 for a detailed dataset to a typical pixel size of 0.5 to 0.75mm. Best segmentation results were achieved for 2 mm thick reconstructed slices of 1 mm spacing. The collimation of the 4-detector CT scanner was mostly set to 2.5 mm, better results were achieved for 1 mm. The first three datasets are shown in a 3D view in Figure 1.

A typical outer vessel shape is circular or slightly elliptical. If *calcification* is present, it is situated *in the vessel* and the inside profile becomes considerably irregular. The densities are measured by CT in Hounsfield Units (HU). In our CTA datasets, the vessel blood with a contrast agent has the densities varying from 150 to 260 HU, the non-calcified plaque has about 80 HU and the calcified plaque deposits about 320 HU–1500 HU.

The vessel density distribution in a manually selected vessel in the left leg (see Figure 2) shows two large dropdowns in the density values, above the knee (slices 380–530) and in the upper part close to the hip (slices 685–741). These decreases of the contrast agent concentrations are caused by two stenoses, which drastically reduce the blood flow and therefore also the concentration of the contrast agent. The blood flow is spread into small collateral vessels. Below the large stenosis above the knee, blood returns to the vessel and the concentration increases back. In fact, it is even higher, since the contrast agent cumulates its concentration here.

To get a clearer picture of how the vessels are represented in the datasets see [8], more details about one of the datasets can be found in[7].

3. Vessel Segmentation Methods

In this section we summarize the knowledge obtained from the literature review on the topic of vessel segmentation. The goal is a robust method for the vessel segmentation from CTA datasets. Since only few technical articles using this modality for a vessel display were found, this section collects everything about segmentation of vessel objects obtained until now, describes the principles and tries to depict problematic steps of each method. Most of the methods described in studied articles deal with DSA (digital subtraction angiography) and MRA (magnetic resonance angiography).

For details about the methods read this section, for discussion about their applicability in the task of 3D vessel segmentation see Section 4.

3.1. Threshold-morphological method

The outline of this section results from personal communications with Miloš Šrámek from the Austrian Academy of Sciences. As already mentioned in Section 2, both tissues of interest, namely vessels and calcifications, overlap in their CT density range with bone tissue. Therefore, a technique capable of independent labeling of all three tissue types is

necessary. In general, two complementary strategies can be followed: An indirect one, in which the bone tissue is identified and removed from the CT data by means of masking. In this case vessels and calcifications remain the tissues with the highest voxel density, which enables a straightforward application of subsequent processing and visualization techniques. And a direct one, in which the vessels and calcifications are segmented and labeled from the original data.

Šrámek prefers the indirect approach since bones are much thicker objects than vessels and, therefore, their segmentation is less sensitive to imaging artifacts (partial volume effect), and bone segmentation errors do not have so dramatic consequences as the segmentation of vessels can have (e.g., missing vessel segments).

According to the nature of the CTA data, Šrámek recommends a thresholding, supplemented by morphologic operations and a connected component labeling as the most promising segmentation technique.

3.2. Wave vessel tracking

The application area of Wave algorithm is vessel tracking in CTA, MRA (vessels of liver).

Cornelia Zahlten described the Wave vessel tracking algorithm in her PhD thesis[26]. She mentioned two approaches and used the second one:

I. Hysteresis thresholding with skeletonization and symbolic graph [11, 21]. Object pixels are selected by hysteresis thresholding: The histogram is divided into three parts—object, background, and overlapping part. Pixels from the overlapping part are added to the object only if they are connected to object pixels. The object is then skeletonized by erosions and the distance transformation is then computed to determine the diameter of the vessels. Finally, a symbolic description via a graph is constructed, where the vessel bifurcations and vessel ends are represented as nodes and the vessel segments as links of the graph.

II. Region growing with simultaneous graph generations [26].This is a region growing approach enriched by bifurcation detection and vessel graph generation. At first, a seed point is put interactively near the root of the vessel tree. Then, the wave goes through the object. The wave is a connected list of voxels belonging to the vessel that have been added in the current step. Until now it is a normal flood-fill algorithm with 26-connectivity voxels, each voxel remembers where the wave has come from (26 binary labels) and the wave direction correction can be applied for high curvature vessels.

The major difference to the classical region growing is in the bifurcation detection and the simultaneous graph construction. If the voxels in the wave (newly added voxels in current step) are not mutually connected, the bifurcation (n-furcation) is detected and an appropriate number of nodes (one for each branch) is created and inserted to the graph. The new wave parts are sorted according to the number of voxels and processed from the largest to the smallest one. This results in the construction of the vessel tree in a top-to-bottom order. Each new branch gets a new label, except for the largest one (75% of the current wave), which holds the current label. During the visualization step each label is assigned a different color to show the hierarchy in the vessel tree.

For a correct branch detection (to avoid over-branching in places with a high vessel curvature), the wave correction is necessary to assure the next wave step would be perpendicular to the actual vessel diameter. Details in [25, 26].

3.3. Vessel enhancement and tracking

The application area is vessel segmentation of abdominal and carotid arteries in MRA.

The principle of this three stage algorithm ([9, 10], similar approaches [14, 18, 19, 22]) is at first to do a preprocessing of the dataset by a 3D filter (vesselness operator V), which enhances tubular structures, then to track the tubular structures in 3D space by finding the path with a minimal cost, which goes through the centerline of the vessels, and finally to detect the vessel borders.

The vesselness enhancement filter V of Frangi et. al. [10] is based on the eigenvalues of a Hessian matrix (a matrix of partial secondary derivatives) evaluated in each pixel of the image in different scales σ. Its response is maximal when the scale of the operator matches the size of the vessel. Therefore the operator simultaneously depicts the vessel size.

For each voxel, the filtering is done in different scales $\sigma \in \langle \sigma_{min}, \sigma_{max} \rangle$ as follows: After computation of the eigenvalues, they are ordered so that $|\lambda_1| < |\lambda_2| < |\lambda_3|$. The respecting eigenvectors $\vec{u}_1, \vec{u}_2$ and $\vec{u}_3$ then point out the singular directions: $\vec{u}_1$ along the vessel, and $\vec{u}_2$, $\vec{u}_3$ the directions in an orthogonal plane. The value of the vesselness operator $V(\mathbf{x}, \sigma)$ is than computed and the highest response over the scales is reported as the response of the vesselness filter $V(\mathbf{x})$. The scale σ where $V(\mathbf{x}, \sigma)$ reaches its maximum determines the size of the vessel with center in voxel $\mathbf{x}$.

The value of vesselness operator $V(\mathbf{x}, \sigma)$ for a given scale σ in voxel $\mathbf{x}$ is for brighter vessels in the darker environment defined as:

$$\begin{aligned} V(\mathbf{x}, \sigma) &= 0 && \dots \text{ if } |\lambda_2| > 0 \text{ or } |\lambda_3| > 0, \\ &= [1 - \exp(-R_A^2/2a^2)] \exp(-R_B^2/2b^2)[1 - \\ &\quad \exp(-S^2/2c^2)] && \dots \text{ otherwise.} \end{aligned}$$

The operator consists of three parts normalized to have the response in interval $\langle 0, 1 \rangle$:

- Anisotropy term $R_A = |\lambda_2|/|\lambda_3|$ should be close to 1 (reflects the cross-sectional symmetry).

- Blobiness $R_B = |\lambda_1| / \sqrt{|\lambda_2||\lambda_3|}$ should be small.
- Degree of image content
  $S = \sqrt{|\lambda_1|^2 + |\lambda_2|^2 + |\lambda_3|^2}$ should be large.

Parameters a, b, c tune the sensitivity of the filter to deviations in R_A, R_B and S. Typical values used in [10] are $a = b = 0.5$ and $c =$ one half of the maximal Frobenius norm of the Hessian matrices, i.e., one half of the length of the vector of lambdas $(\lambda_1, \lambda_2, \lambda_3)$. Another possibility is to use a normalization by the maximal intensity $0.25\sigma^2 I_{max}$.

The operator enhances the tubular structures, filters out blobs and plateau-like structures, but also reduces the vessel diameter, has dropouts at bifurcations (detects them as to be plate-like) and is highly sensitive to bones and calcifications in CTA datasets.

After filtering by a vesselness operator, the vessel centerline is detected by 3D snakes and modeled by B-spline curves, then the vessel wall is segmented and modeled by a tensor product B-spline surface.

3.4. Real time vessel enhancement

The application area is real-time segmentation of DSA images. The principle of this method published by Poli and Valli [16, 17] is similar to the approach of Frangi et al. (see Section 3.3). Both use Gaussian filters in different scales for vessel enhancement. Cagnoni et al. [1, 2] applied then a genetic algorithms optimization. The main points of Poli and Valli's algorithm are:

- Application of *directional filters* with different half-widths w and half-lengths l $(= k\sigma,\ k = 1, 2, \ldots)$.
- *Separation of the Gaussian filter* computation into *atomic filter computations*, to achieve a *real-time response* (convolution is a linear operation, so a convolution with a big kernel can be done by addition of the results of convolutions from two smaller filters,...).
- Application of a *validation step to ignore the response to step edges*—the filter response is accepted if also two pixels in the distance $\pm v$ perpendicularly to $\vec{n}$ are outside of the vessel, i.e., have lower values than a central pixel. The distance v should be larger then the largest structure of interest. This step removes negative values near the vessel borders and noise, but also thin vessels after branching from the thick ones.
- Hysteresis thresholding of the validated images helps if the noise is too high.

To reduce the filtering artifacts, the authors decompose the directional derivatives not only in two directions but in four $\vec{n} = [1,0], [0,1], [\frac{\sqrt{2}}{2}, \frac{\sqrt{2}}{2}], [\frac{\sqrt{2}}{2}, -\frac{\sqrt{2}}{2}]$ and as a result, they take a maximum response over all $\vec{n}, w, l$. According to their test image, where the best parameter setting was $\sigma = 1, w = 2, l = 2$, it seems that *no* integration over set of scales is necessary!

3.5. Direct vessel tracking in 3D

The application area is CTA of abdominal aorta and MRA.

Wink et al. [24] described an interactive segmentation method, which works locally, without preprocessing of the whole dataset and needs about 10s per vessel. The user selects two start-points A and B in the thick part of a vessel and runs the tracking algorithm. The points give a possible direction of the vessel centerline $\vec{a} = B - A$. The method estimates the position of the next candidate point C in the direction of vector $\vec{a}$, in the distance b based on the current minimal vessel diameter d_{min}. Precisely $b = \alpha d_{min}$, where α is a given constant.

Then the precise position of a new point C_{new} is computed. In the square surroundings of the candidate point C, which is perpendicular to the vessel axis direction $\vec{a}$, they compute for each point the likelihood that it is a center point of the vessel. This is done by casting of a fan of rays from each point in the square. Each ray ends at voxel that localy looks as the vessel border. Then, they detect the most possible vessel center point C_{new} in this square and store this new position as a new centerline end. It becomes the part of up-to-now detected vessel and a new candidate point is generated in the computed axis direction. The estimated point C need not to lie inside of the vessel—it is sufficient when the true vessel center lies in the square around it [24, Fig. 8]. The size s of this square is computed as $s = \beta b$, where β is another given constant.

The center likelihood is computed as follows: For each pair of rays in opposite directions the likelihood of being-a-center is computed as a ratio of the shorter to the longer of the distances to the vessel border. The border is detected as a falling gradient in the same direction as the direction of the ray. This has an advantage since using this approach the border of bright vessel or the end of calcification is found.

The authors also proposed a possibility to *force a search direction* to the central vessel direction, to *limit the curvature of a vessel* by a coefficient and to *search a whole tree* of possible vessels and continue in the direction of the highest sum of center likelihoods. They also proposed an approach, which is based on the same principle as our modification of the live wire method (see Section 4.6)—namely to define start- and end-points and to find the vessel centerline by the use of the dynamic programming or tree search. The more points are defined, the more the searched data space is reduced. A similar tracking approach called *imaginary catheter* was published as a work in progress by Verdonck et al. [23].

3.6. Live wire and Intelligent scissors

The application area is a boundary segmentation of any object.

The *live wire* (LW) method [5, 6] was originally designed for a 2D interactive segmentation of *boundaries* in difficult images with faint signal of boundaries or even gaps in boundaries, for objects with similar boundary properties around them, and for regions distorted by noise. In general, it speeds-up the user interaction by interactive offering the boundary segments between the user defined start-point and the current position of the cursor. After selection of the end-point of the segment, it becomes a new start-point and the whole process of boundary segment selection starts from this new point.

The fundamental ideas of this method and the name *live wire* were developed in cooperation of groups around Udupa and Barrett. But then (1995/96), the development continued independently and Mortensen and Barrett [15] introduced the name *intelligent scissors*. The important principles used by Falcao et. al. [5] are:

The boundary is an oriented, closed and connected planar contour. It is formed from a subset of oriented edges such that the sum of the costs of these edges is minimal. The oriented pixel edge is defined between each pair of four-adjacent pixels. The oriented pixel edge element, which is a part of the boundary, is called *bel*, a boundary element. Each bel $b = (q,r)$ has its location (between pixels q and r) and orientation (such that q is always inside the boundary). Each bel b is assigned a $cost(b)$, computed from the selected set of bel features. Details about the computation of the costs, about the possible training phase and also the explanation of the relation to intelligent scissors [15] are given in [6]. Pixels and bels form nodes and arcs of a weighted directed graph. A modified Dijkstra's minimal cost path algorithm is used.

For speeding up of the interaction times, Falcao et al. [5] proposed a method called *live wire on the fly* (LWOF), which computes the paths "on demand" according to the cursor position.

3.7. Knowledge-based 2D approach

The application area is segmentation of vessels in DSA.

The development of a hierarchical heuristic method for a knowledge-based vessel segmentation from projections in subtraction angiography was started by Cleynenbreugel et al. [3], and continued in [4, 20]. The method applies a rule-based system and segments the blood vessels via a multi-stage approach.

The proposed multi-layered image representation [20] has the following layers: Pixels $\rightarrow$ line segments $\rightarrow$ vessel parts $\rightarrow$ vessels $\rightarrow$ anatomically labeled vessels.

An important aspect is the splitting of large amount of available heuristic knowledge into separate blocks, which simplifies integration of new heuristic models. Also the feedback strategy, which allows re-computation of missing attributes and the updating of interpretation labels makes the method more robust.

4. Applicability of the Methods

In this section, we describe our experience with the algorithms described in Section 3 and collect our opinions about the applicability of described methods to the task of vessel segmentation in CT angiography datasets. Up to now, our implementations of four algorithms were tested: Threshold-morphological method (Section 4.1), wave vessel tracking (Section 4.2), 2D version of vessel enhancement (Section 4.3), and a live wire (Section 4.6). Therefore, about the other methods only opinions are mentioned, which are not supported by precise algorithm evaluation.

4.1. Tests of threshold-morphological method for bone removal

The bone removal is very usefull mainly for the visualization using a maximum intensity projection (see Figure 4). If used as a preprocessing step for vessel segmentation, incorrectly removed vessel parts may appear, caused by the applied thresholding. The following vessel segmentation algorithm may then suffer from false detected stenoses and from a problem of jumping over gaps in the data. The distort vessel shape would also affect the following measurements.

A combined bone segmentation and removal method, which uses a two-phase thresholding and region growing followed by average-value and region-size based labeling, was tested with very promissing results [12, 13]. The method works in slabs to achieve interactivity. The method cannot handle variations of intensities in the bone automatically and has to allow a user interaction, as carefull settings of the segmentation parameters is still often necessary.

4.2. Tests of vessel tracking by Wave

A simplified version of this approach with an adaptive thresholding by means of bimodal histogram without a curvature correction was implemented. Before application of this algorithm, it is necessary to enhance the contrast between the vessel and the background by setting of a correct windowing (to select only an interval of data values).

The algorithm without branching corrections was tested at the beginning of the bibliography search. A two-step segmentation was used: At first, the vessel surrounding was masked out by the interval selection and then the vessel

tracking itself was performed. The masking of the volume had the comparable effect as the process of windowing.

The algorithm was successful for the parts of the leg starting below the knee and ending at the lower part of the body if the windowing/masking isolated all the bridges to the surrounding tissues (The simplest dataset was No. 2 which has higher resolution—see two right panels in Figure 3). The algorithm stopped very often in small vessels in the lower part of the foot as the vessel was no more homogeneous enough due to the noise and maybe the partial volume artifact (see Figure 3 left). Also if the vessel touched the bone in the abdomen or if a star-like reconstruction artifact was present, it spread into the surrounding tissue or even filled up the whole 3D dataset. Another important disadvantage was a non-predictable erosion of the detected vessel caused by ignoring the voxels out of the windowing interval.

Figure 3. Datasets No. 1 (left) and 2 (right) and segmented vessels

We suspect that the windowing, which is necessary to achieve any meaningful result, can suppress the adaptive thresholding to minimal influence and can cause an unpredictable erosion of the detected vessel. The detection of small vessels is then very hard (see limited length of vessels in the left panel in Figure 3) and the algorithm without branching corrections reduces itself back to the region growing. Also due to a very low interactivity and many fails caused by the locality of the algorithm it was realized not to continue in testing and not to use this algorithm for the project.

4.3. Test of vessel enhancement

The algorithm has been developed for MRA vessel segmentation where no signal from bone is present, and especially for abdomen, where the vessels have a large diameter. As bone is present in the CTA datasets, the approach cannot be applied directly.

But the 3D filtering step, which enhances tubular structures of diameter from a given interval and even detects the vessel diameter, can be used in two places: In the modification of the live wire vessel tracking (see Chapter 4.6) as a supporting feature helping in the detection of ”being in the vessel”, or as a post-processing step for a precise positioning of the detected path (e.g., the minimal path) to obtain a true centerline of the vessel.

For large diameters the vesselness method is precise enough (carotid arteries). For small vessels of diameter of 2–3 voxels (like in brain or foot), the Hessian is not computed in the correct centers of the vessels, but in the centers of sampled voxels, and the variation of anisotropy term $R_A = |\lambda_2|/|\lambda_3|$ is therefore too high [14].

2D tests showed that the operator enhances the vessels of the selected diameter. But it also turned out that the image has to be extended to omit false edge responses on the borders, which slows down the filtering.

Frangi et al. used snakes for the vessel extraction from the vesselness data. It should prefer detection of smooth vessel centerlines, i.e., should work globally in a local neighborhood. This may be useful for jumps over bifurcations or calcifications.

4.4. Real-time vessel enhancement

This algorithm differs from the Frangi’s vessel enhancement by application of different derivative kernels, with different width w and length l. The authors also use integer arithmetic and a sophisticated decomposition of the kernels into addition of a large number of responses of only 2-pixel kernels, which results in a real-time vessel segmentation.

Surprisingly, Poli et al. do not use the kernels over the range of scales σ but only for $\sigma = 1$! Also the best compromise values of $\sigma = 1, w = 2, l = 2$, seem to be relatively strange, as they negate the scale-space approach.

The ideas of optimal computation of the convolutions are inspirative and should be in mind if any filtering approach will be applied.

4.5. Direct vessel tracking

This method is the only one in this paper that was directly applied to CTA data. It seems to be very interesting, as it does not search the whole data volume but only the promising part, where the vessel should be located. It also handles the calcifications in CTA with a correct estimate of the *outer* border of calcifications, ignores perpendicularly outgoing vessels as they have a low contribution to the likelihood, selects one vessel in bifurcations (no wrong turnings or leaving of the vessel), and estimates the vessel diameter.

On the other hand, the method was used for vessels with a large diameter in abdomen, which is not our case. Also the

necessity of permanent user interaction may be a drawback in the large datasets. It needs a simultaneous visualization and a specialized user interface.

4.6. Tests of modified Live wire

We have proposed a modification [13] of the original algorithm in order not to search the *boundary* but the path through a *homogeneous region* in a given window of values. That means the *path through the vessel*.

The proposed modification needs an interactive selection of a start-point and a set of end-points: the start-point in the abdominal aorta and the end-points at the ends of the tracked vessels. Then, the shortest path search between the start-point and all the points in the image (graph) is performed. The algorithm prefers homogeneity (smallest difference of values) and jumps out of the given window are highly penalized (to prevent tracking in the false, but homogeneous regions of different tissues). The algorithm works very intuitively, the user interaction is concentrated to the beginning of the session, which saves time of the operator. After the processing of the dataset, the paths between start and all end-points are drawn. At this point, any shortest path from the start-point to any other end-point can be found interactively.

The algorithm was tested on 2D and 3D datasets with promising results. It detects vessels with a high probability of success (see an example of curved planar reformation generated from one detected vessel in the right panel of Figure 4). On the contrary, a non-optimized version needs a large amount of memory, which is now solved by swapping to disk. Also a modification of any point inside the vessel means the setting of this point as a starting one and the complete re-computation of the shortest path (sub-)tree. The graph parameters are fixed, i.e., no tuning according to the dataset via a teaching phase is supported.

4.7. Knowledge-based approach

This approach was not tested, i.e., only some notes follow.

Cleynenbreugel/Smets processed the 2-dimensional DSA datasets and used a thin-vessel detection by the maximal image-intensity detector. This detector is not applicable to CTA, as the whole 3D dataset is processed and no 2D MIP of vessels exists. The approach seems to be robust, as it combines a bottom-up approach with a feedback based recalculation and re-labeling and applies not only the geometrical but also the anatomical knowledge. On the other hand, segmentation of the whole 3D CTA datasets is more simple as it does not need to deal with overlapping and crossing of vessels caused by a 2D projection of a 3D object (as in DSA).

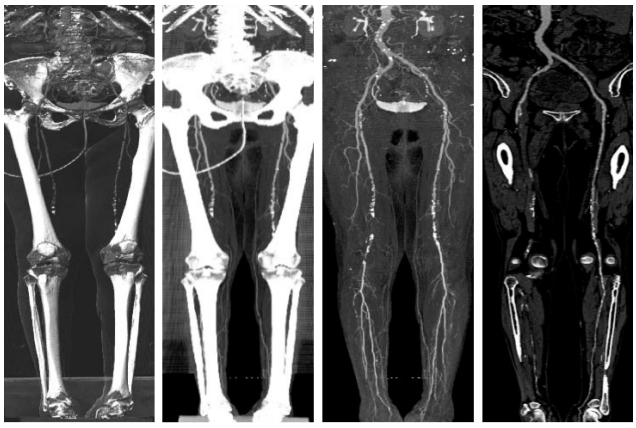

Figure 4. Dataset No. 8: Direct volume rendering, MIP with bone, MIP without bone, and Curved Planar Reformation of one vessel

5. Conclusions

The paper summarized the information about angiography datasets acquired by a spiral CT scanner and about the appearance of vessels of interest in these datasets. Then it described seven methods for segmentation of vessels in medical datasets found in literature and discussed their applicability to the task of CTA vessel segmentation.

The *thresholding-morphological method* was not usable for vessel segmentation, but was advantageously applied for bone removal for MIP visualization. *Wave vessel-tracking* was too slow for large datasets with lower reliability in comparison to the shortest-path search between given pairs of points. *The vessel enhancement method* enhanced bone more than vessels in CTA datasets. But it can be used as a supporting feature for vessel centerline detecion. We assume that the *real-time vessel enhancement* would work similarly as the vessel enhancement method. The principles used in *direct vessel tracking* were used for vessel centerline detection and not for vessel tracking itself, mainly as the lower extremity arteries have a substantially smaller diameter and also the user interaction cannot be concentrated to the beginning of the session. The *knowledge based method* was too specialized for 2D case, which is not necessary in case of CTA. The most promising approach is the modification of the *live wire method* for vessel detection.

After the tests, we have decided to use two methods; a bone removal for MIP projection generation and the combination of approaches of live wire and direct vessel tracking for vessel and its centerline detection. Preliminary results have already been published in [12] and [13]. In the future we will concentrate on tuning of the implemented methods and tests in the clinical environment.

Acknowledgments

This work was done in the VRVis research center, Vienna (*http://www.vrvis.at*) and in TIANI MedGraph GmbH, (*http://www.tiani.com*). Dataset courtesy D. Fleischmann, AKH Vienna. Special thanks to E. Gröller, D. Fleischmann, D. Sandner, M. Šrámek and M. Čapek for valuable discussions, and to the referees, whose comments considerably improved the presented text.

References

[1] S. Cagnoni, A. Dobrzeniecki, R. Poli, and J. Yanch. Genetic algorithm-based interactive segmentation of 3D medical images. *Image and Vision Computing*, 17(12):881–896, 1999.

[2] S. Cagnoni, A. B. Dobrzeniecki, R. Poli, and J. C. Yanch. Segmentation of 3D medical images through genetically-optimized contour-tracking algorithms. CSRP-97-28, University of Birmingham, School of Computer Science, 1997.

[3] J. V. Cleynenbreugel, F. Fierens, C. Smets, P. Suetens, and A. Oosterlinck. Knowledge-based segmentation of subtraction angiograms. In *IPMI'87*, pages 307–314, Utrecht, The Netherlands, June 22–26, 1987.

[4] D. Delaere, C. Smets, P. Suetens, G. Marchal, and F. V. de Werf. A knowledge-based system for the 3D reconstruction of blood vessels from two angiographic projections. In J. Cornelis and S. Peeters, editors, *Proceedings of North Sea Conference on Biomedical Engineering*, page 11 pages, Antwerp, Belgium, Nov. 19–22, 1990.

[5] A. X. Falcao, J. K. Udupa, and F. K. Miyazawa. An ultra-fast user-steered image segmentation paradigm: Live wire on the fly. *IEEE T. on Med. Imag.*, 19(1):55–62, Jan. 2000.

[6] A. X. Falcao, J. K. Udupa, S. Samarasekera, S. Sharma, B. E. Hirsch, and R. A. Lotufo. User-steered image segmentation. *GMIP*, 60:233–260, 1998.

[7] P. Felkel. Segmentation of vessels in peripheral CTA datasets. VRVis Center Technical report TR-VRVis-2000-008, Austria, *www.vrvis.at*, Dec. 2000.

[8] P. Felkel and R. Wegenkittl. Vessel tracking in peripheral cta datasets – an overview. In T. L. Kunii, editor, *SCCG'2001*, pages 269–278. Comenius University, Bratislava, Slovakia, Apr. 2001. (Held in Budmerice, Slovakia).

[9] A. Frangi, W. Niessen, R. Hoogeveen, T. van Walsum, and M. A. Viergever. Model-based quantitation of 3D magnetic resonance angiographic images. *IEEE Transactions on Medical Imaging*, 18(10):946–956, 1999.

[10] A. Frangi, W. Niessen, K. Vincken, and M. Viergever. Multiscale vessel enhancement filtering. In W. Wells, A. Colchester, and S. Delp, editors, *MICCAI'98*, volume 1496 of *LNCS*, pages 130–137. Springer-Verlag, Germany, 1998.

[11] G. Gerig, T. Koller, G. Székely, C. Brechbuhler, and O. Kubler. Symbolic description of 3-D structures applied to cerebral vessel tree obtained from MR angiography volume data. *LNCS*, 687:94–111, 1993. Cited according to [26].

[12] A. Kanitsar. Advanced visualization techniques for vessel investigation. Master's thesis, TU Vienna, 2001.

[13] A. Kanitsar, R. Wegenkittl, P. Felkel, D. Sandner, E. Gröller, and D. Fleischmann. Automated vessel detection at lower extremity multislice CTA. In *European Radiology*, volume 11(S1), page S236. Springer Verlag, Heidelberg, Germany, 2001. Presented at ECR'2001, Vienna, Austria.

[14] K. Krissian, G. Malandain, N. Ayache, R. Vaillant, and Y. Trousset. Model based detection of tubular structures in 3D images. RR-3736, INRIA, Sophia Antipolis, July 1999.

[15] E. N. Mortensen and W. A. Barrett. Intelligent scissors for image composition. In *SIGGRAPH'95*, pages 191–198, Los Angeles, CA USA, Aug. 6–11, 1995.

[16] R. Poli and G. Valli. Efficient enhancement and segmentation of blood vessels by integration of multiple directional filters. Technical Report 940701, Department of Electronic Engineering, University of Florence, Italy, July 1994.

[17] R. Poli and G. Valli. An algorithm for real-time vessel enhancement and detection. *Computer Methods and Programs in Biomedicine*, 52:1–22, Nov. 1996.

[18] Y. Sato, S. Nakajima, H. Atsumi, T. Koller, G. Gerig, S. Yoshida, and R. Kikins. 3D multi-scale line filter for segmentation and visualization of curvilinear structures in medical images. In *Proc. First Joint Conference of CVRMed II and MRCAS III*, pages 213–222, Grenoble, France, 1997.

[19] Y. Sato, C.-F. Westin, A. Bhalerao, S. Nakajima, N. Shiraga, S. Tamura, and R. Kikins. Tissue classification based on 3D local intensity structures for volume rendering. *IEEE Trans. on Visualization and Computer Graphics*, 6(2):160–180, Apr.–June 2000.

[20] C. Smets. *A knowledge-based System for the Automatic Interpretation of Blood vessels on Angiograms*. PhD thesis, Katholieke Univesiteit Leuven, 1990.

[21] G. Székely, T. M. Koller, R. Kikinis, and G. Gerig. Structural description and combined 3-D display for superior analysis of cerebral vascularity from MRA. In *Visualization in Biomedical Computing*, volume 2359, pages 272–281, 1994. Cited according to [26].

[22] D. Vandermeulen, C. Smets, P. Suetens, G. Marchal, J. Gybels, and A. J. Oosterlinck. Knowledge-based 3-D segmentation of blood vessels on a spatial sequence of MRI and ultrasound images. In S. J. Dwyer, R. G. Jost, and R. H. Schneider, editors, *Medical Imaging III: Image Processing*, volume 1092 of *Proc. SPIE*, pages 142–148, 1989.

[23] B. Verdonck, I. Bloch, H. Maitre, D. Vandermeulen, P. Suetens, and G. Marchal. Blood vessel segmentation and visualization in 3D MR and spiral CT angiography. *Computer Assisted Radiology*, pages 177–182, 1995.

[24] O. Wink, W. Niessen, and M. Viergever. Fast delineation and visualization of vessels in 3-D angiographic images. *IEEE Trans. on Medical Imaging*, 19(4):337–346, Apr. 2000.

[25] C. Zahlten. Reconstruction of branching blood vessels from CT-data. In M. Göbel, H. Müller, and B. Urban, editors, *Visualization in Scientific Computing*, pages 41–52. Springer-Verlag, Wien, 1995.

[26] C. Zahlten. *Beiträge zur mathematischen Analyse medizinischer Bild- und Volumendatensätze*. PhD thesis, Universität Bremen, 1995.